

## Paper:

# Simulation of Slope Failure Distributions Due to Heavy Rain on an Island Composed of Highly Weathered Granodiorite Based on the Simple Seepage Analysis

Takatsugu Ozaki<sup>\*1,†</sup>, Akihiko Wakai<sup>\*1</sup>, Go Sato<sup>\*2</sup>, Takashi Kimura<sup>\*3</sup>, Takanari Yamasaki<sup>\*4</sup>, Kazunori Hayashi<sup>\*5</sup>, and Akino Watanabe<sup>\*1</sup>

<sup>\*1</sup>Graduate School of Science and Technology, Gunma University  
1-5-1 Tenjincho, Kiryu, Gunma 376-8515, Japan

<sup>†</sup>Corresponding author, E-mail: t15807002@gunma-u.ac.jp

<sup>\*2</sup>Graduate School of Environmental Informations, Teikyo Heisei University, Tokyo, Japan

<sup>\*3</sup>Graduate School of Agriculture, Ehime University, Ehime, Japan

<sup>\*4</sup>Japan Conservation Engineers & Co., Ltd., Tokyo, Japan

<sup>\*5</sup>Okuyama Boring Co., Ltd., Miyagi, Japan

[Received November 30, 2020; accepted March 10, 2021]

To fully and rapidly develop a real-time early warning judgment system for slope failure at the time of heavy rains including overseas, it is necessary to predict water movement in the soil at the time of rainfall. In addition, to apply the system to a place where insufficient geotechnical and geological data have been amassed, it is necessary to evaluate the risk of slope failure based on physical properties obtained from a simple soil test. Therefore, in this study, the authors set Gogoshima Island in Ehime Prefecture as a study site and evaluated the water movement over time in the soil during heavy rain using a simple prediction equation of rainfall seepage process. Soil properties were determined through simple in-situ and laboratory tests. As a result, it was found that the factor of safety for slope failure in the head and wall of a valley dissecting the hillside slope composed of granodiorite in which weathering has progressed can be planarly evaluated using the simple prediction equation.

**Keywords:** simulation of slope failure distributions, highly weathered granodiorite (saprolite), simple seepage analysis, Gogoshima Island

## 1. Introduction

Japan, which is located in a warm and humid climate and has a large mountainous land area, has a problem of slope failure. Therefore, the Japan Meteorological Agency has calculated the soil water index (Okada et al. [1]) using the series three-stage tank model of Ishihara and Kobatake [2], and evaluated and predicted risk of landslide-related incidents caused by heavy rain. However, the proportional constants such as the runoff coefficient set in each tank hole are subject to the con-

dition that there are sufficient observation results such as the runoff amount for calibration targets. In addition, the geological data etc. to constitute the basis for setting each coefficient are exhaustively required. On the other hand, as proposed by Okimura et al. [3], the number of proposals for risk assessment using weather radar data has been increasing in recent years. There is a global trend of using distributed hydrological analyses to track the flow of rainwater and assess the risk of slope failure, such as Lima Neves Seefelder et al. [4] and Shi et al. [5]. However, in the case of performing a precise calculation for a wide area, in particular a saturated-unsaturated seepage flow analysis, a high-performance computer is required, and adequate time is needed for the calculation. There are problems such as failure to obtain sufficient measures of the physical properties and initial conditions of soil to meet the strictness of the method. With this background, to fully and rapidly develop a real-time early warning judgment system for slope failure at a time of heavy rain including overseas, it is necessary to predict water movement in the soil at the time of rainfall as in Wakai et al. [6] and Ozaki et al. [7]; and it is also necessary to evaluate the risk of slope failure by adopting the physical properties obtained from a simple soil test.

Therefore, the authors have evaluated the water movement in the soil over time during heavy rain using a simple prediction equation of rainfall seepage process proposed by Ozaki et al. [7] and have attempted to planarly evaluate the factor of safety based on the soil properties obtained from simple in-situ and laboratory tests. As the test site, the authors set Gogoshima Island, Ehime Prefecture (**Fig. 1**), where a large number of shallow landslides occurred in July 2018 due to heavy rains. About **Fig. 1**, shown in red is the distribution of shallow landslide (including flow-down and erosion areas) caused by the July 2018 heavy rains (the shallow landslide distribution, the data of Sato et al. [8] were used), for the fundamental fig-



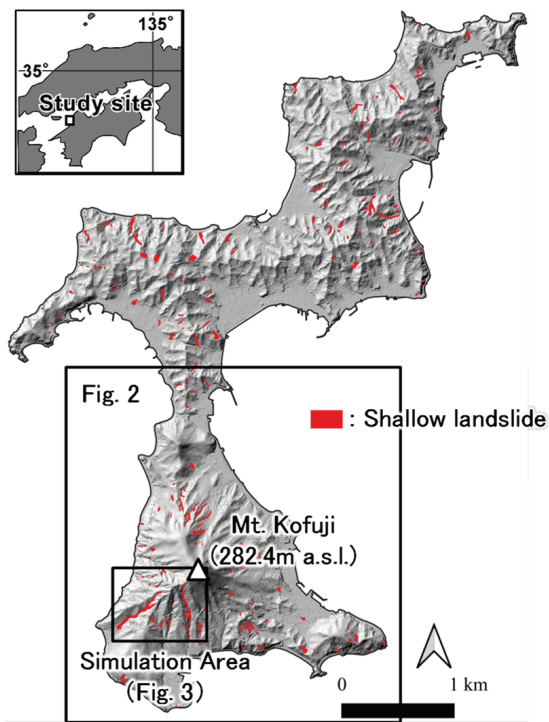


**Fig. 1.** Test site (Gogoshima Island, Matsuyama City, Ehime Prefecture).

ure, the shadow map created from the 0.5 m mesh DEM of the aerial laser survey measured by Forestry Agency [9] in 2018 was used.

## 2. Outline of Study Site

Gogoshima Island has an area of 8.76 km<sup>2</sup>, and to the south of the island is the conical Mt. Kofuji with an elevation of 282.4 m (**Fig. 1**). The July 2018 heavy rains caused many shallow landslides in citrus on-site, resulting in huge damage (Sato et al. [8]). In particular, a shallow landslide occurred along the valley dissecting Mt. Kofuji, destroying infrastructure with the debris flow. The geology is mainly composed of Cretaceous granodiorite and Miocene andesite, with landslide and beach deposits distributed in some areas (**Fig. 2**). About **Fig. 2**, the geological map was created based on 1/50,000 surface layer geological map “Mitsuhamma” [10], for the fundamental figure, the shadow map created from the 0.5 m mesh DEM of the aerial laser survey measured by Forestry Agency [9] in 2018 was used.

## 3. Various Test Methods to Determine Soil Properties and Simple Prediction Method of Rainfall Seepage Process

### 3.1. Methods of In-Situ and Laboratory Tests

On August 22 and 23, 2020, an on-site survey in the area that collapsed due to the July 2018 heavy rains was

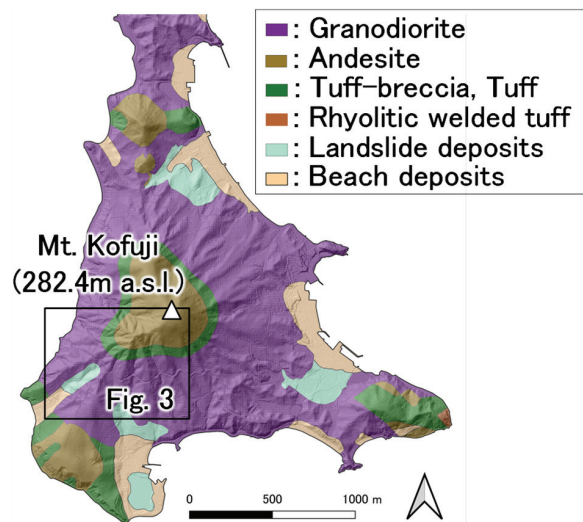


**Fig. 2.** Surface geology of the southern part of Gogoshima Island.

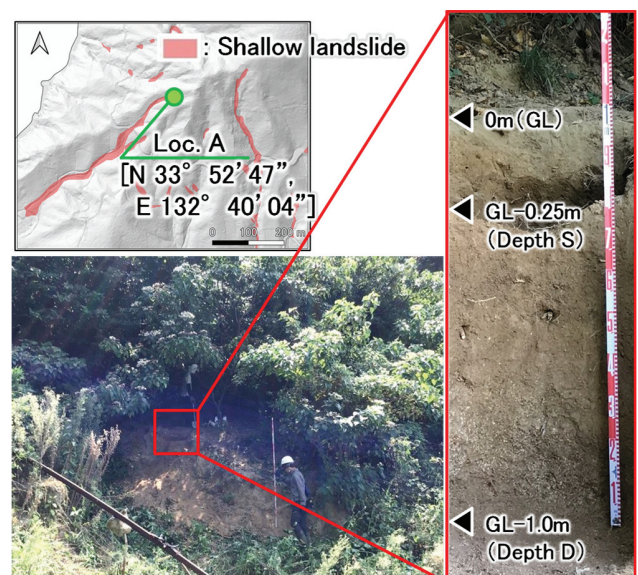


**Fig. 3.** Location of the in-situ test and photograph of the test site.

carried out, and a vane cone shear test using a soil strength probe and an in-situ falling head test using a portable mini disk infiltrometer made by Meter, Inc. were conducted at Loc. A shown in **Fig. 3**. The test site falls on a landslide scarp in the area of shallow landslide as shown in **Fig. 3**. The geology is composed of a granodiorite weathered material (decomposed granite soil) as described later, and its foundation (bedrock) was not found at the site. Therefore, the slip surface was found that was present in the decomposed granite soil. The above in-situ test was conducted by artificially dissecting this scarp and providing steps. The soil strength probe is a tester developed by the Public Works Research Institute that measures the internal friction angle and cohesion on site by measuring both the vertical penetration load and the rotational (shear) torque

of a winged cone (Public Works Research Institute [11]). The portable mini disk infiltrometer can calculate the hydraulic conductivity by placing a hydraulic conductivity disk made by sintering stainless steel at the bottom onto the soil and recording the falling water level.

Looking at the cross section of the soil layer at the test site (Fig. 3), its color is found to change downward from brown to grayish brown around the excavation depth of 1.0 m. It was also confirmed that the particle size was increasingly coarse in the downward direction. The above in-situ test was carried out for drilling depths GL -0.25 m (hereinafter, Depth S) and GL -1.0 m (hereinafter, Depth D). Additionally, an undisturbed sample and a disturbed sample were collected from the horizons of Depth S and Depth D to carry out soil tests (moisture content, wet density, particle size, liquid limit and plastic limit of soil, and density of soil particles) and X-ray diffraction. The latter using the X-ray diffractometer MiniFlex made by Rigaku Corporation owned by Japan Conservation Engineers & Co., Ltd. was carried out.

### 3.2. Summary of Simple Prediction Equation of Rainfall Seepage Process

To evaluate the factor of safety with respect to the slope failure that changes from moment to moment due to heavy rain, a simple prediction equation of rainfall seepage process proposed for a semi-infinite slope of fine sand with relatively small saturated hydraulic conductivity is adopted. Ozaki et al. [7] presented details such as the effectiveness of the simple prediction equation. Therefore, only the theory is extracted and described here.

Assuming a constant rainfall intensity  $I$  (cumulative water column height per unit time), if all the rainwater infiltrates into the ground as it is on a long and large slope with a constant gradient, the falling velocity  $v_{bs}$  [m/h] of the wetting front, which expands downwards as rainwater fills (percolates) into the unsaturated layer, is theoretically given as follows based on the volume of water necessary to saturate the void in the unsaturated layer:

$$v_{bs} = \frac{I}{n \left( 1 - \frac{S_{r0}}{100} \right)}, \quad \dots \quad (1)$$

where  $n$  is the porosity and  $S_{r0}$  is the initial average degree of saturation of the unsaturated layer shallower than the groundwater level.

However, on the assumption of a falling velocity having an appearance slightly different from the theoretical one in practice, it is generalized in this paper by using the following equation, the right-hand side of Eq. (1) multiplied by the correction coefficient  $\beta_v$ .

$$v_{bs} = \frac{\beta_v I}{n \left( 1 - \frac{S_{r0}}{100} \right)}. \quad \dots \quad (2)$$

In a case where the rainfall intensity increases, it is assumed that the amount of rainwater supplied from the ground surface becomes larger than the amount of wa-

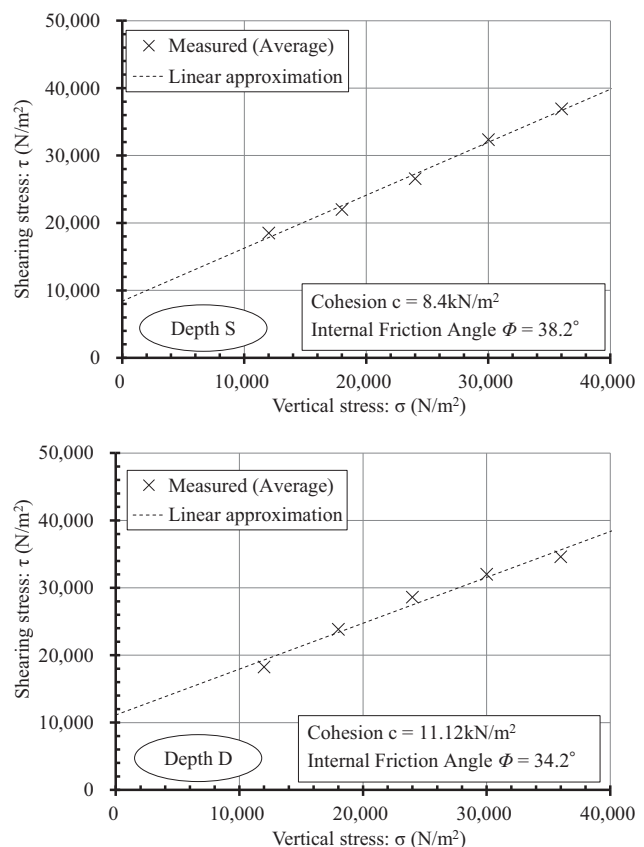


Fig. 4. Relationship between vertical stress and shear stress obtained by vane cone shear test using soil strength probe.

ter moving downwards in the surface stratum, and part of the rainwater cannot infiltrate and as thus flows down the ground surface as it is. Therefore, the intensity of rainfall that cannot infiltrate from the surface into the ground and flows down the ground surface, is defined as the critical rainfall intensity  $I_{cr}$  [mm/h]. To simplify the model, the above proposal focuses only on the vertical component of the rainwater seepage phenomenon and does not consider the horizontal component of the flow.

Ozaki et al. [7] derived the parameters  $\beta_v = 2.05$  and  $I_{cr} = 40$  mm/h of the simple prediction equation as a result of a parametric study on the assumption of fine sand with saturated hydraulic conductivity  $K_s = 1.0 \times 10^{-3}$  cm/s ( $1.0 \times 10^{-5}$  m/s).

## 4. Results of Various Tests to Determine Soil Properties and Planar Evaluation of Factor of Safety with Respect to Slope Failure

### 4.1. Results and Discussions of In-Situ Test

Figure 4 shows the relationship between the vertical and shear stresses obtained from a vane cone shear test using the soil strength probe. The following results were obtained: cohesion  $c$  of Depth S = 8.40 kN/m², internal friction angle  $\phi$  of Depth S = 38.2°, cohesion  $c$  of Depth D = 11.12 kN/m², and internal friction angle  $\phi$  of Depth D



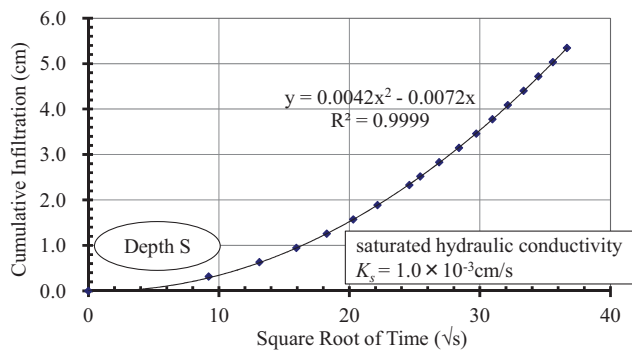


**Fig. 5.** Result of in-situ falling head test using portable mini disk infiltrometer (input conditions set for calculation of  $K_s$  are “Soil Type: Sandy Clay” and “Suction: 2”).

= 34.2°. Since there was little variation in the read values of torque, the average of the values of the test performed three times at each load for evaluation was adopted.

The result of the in-situ falling head test using the portable mini disk infiltrometer is shown in **Fig. 5** (the result for Depth D is omitted). The saturated hydraulic conductivity  $K_s$  of Depth S is estimated to be about  $1.0 \times 10^{-3}$  cm/s, and the saturated hydraulic conductivity  $K_s$  of Depth D is estimated to be about  $2.0 \times 10^{-3}$  cm/s. Regarding the relationship between the test result using a portable mini disk infiltrometer and saturated hydraulic conductivity, Tagawa [12] stated that the same degree of accuracy is obtained as with the saturated hydraulic conductivity calculated using the borehole method. Although the number of tests is considered statistically small in order to verify the accuracy, the result obtained by using the portable mini disk infiltrometer was found to be generally appropriate, as there is no large difference between the value of the saturated hydraulic conductivity obtained from the 20% particle size (Creager method) shown in **Fig. 6** and obtained by using the portable mini disk infiltrometer in Depth S.

#### 4.2. Results and Discussions of Laboratory Test

The results of various laboratory tests are shown in **Table 1** and **Fig. 6**. Since the moisture content  $w$  is in the range of 6–30%, the soil particle density  $\rho_s$  is in the range of 2.6 to 2.8 g/cm³ or close thereto, and the wet density  $\rho_t$  is in the range of 1.5 to 2.0 g/cm³, indicating the characteristics of decomposed granite soil according to the Japanese Geotechnical Society [13]. The plasticity index of Depth S, which has a high clay content, is larger than Depth D, and the consistency is confirmed.

The test results of X-ray diffraction analysis by the random orientation method and the preferred orientation method are shown in **Table 2**, and **Figs. 7** and **8**. About **Fig. 7**, kaolin (Kln) and illite (Ill) were determined by the result of dropping only the clay particles contained in the supernatant treated by hydraulic elutriation method (in a preferred orientation), drying, and measuring by X-ray diffraction. The combination of the minerals and clay minerals of Depth S and Depth D was substantially the

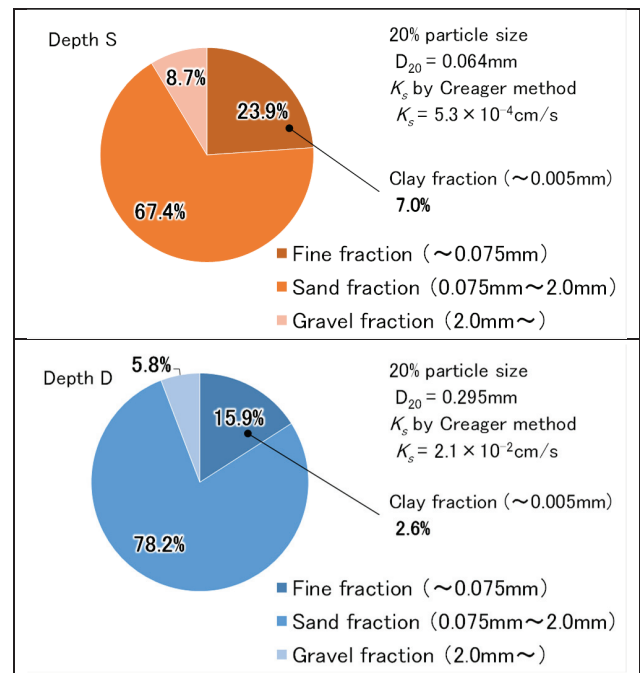


**Fig. 6.** Results of particle size test.

**Table 1.** Result of various laboratory tests on in-situ weathered decomposed granite soil.

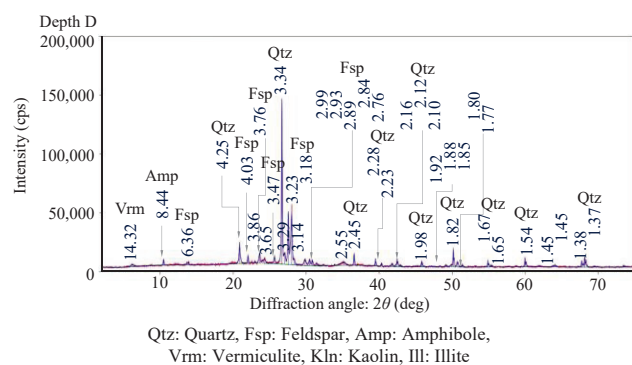
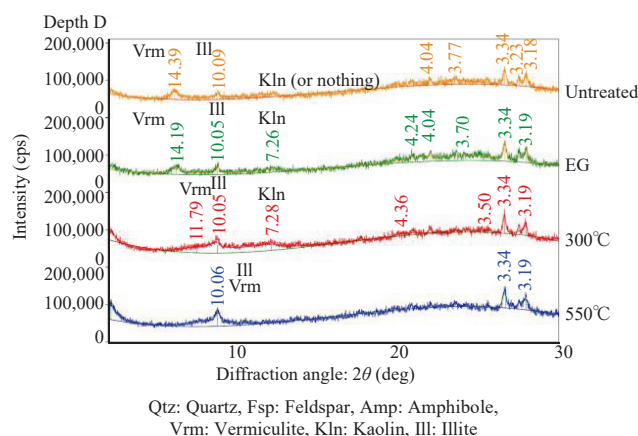
Soil properties	Depth S	Depth D
Moisture content: $w$	13.68%*	9.44%
Wet density: $\rho_t$	1.66 g/cm³	1.66 g/cm³
Dry density: $\rho_d$	1.45 g/cm³	1.52 g/cm³
Average soil particle density: $\rho_s$	2.53 g/cm³	2.62 g/cm³
Liquid limit: $w_L$	36.13%	31.66%
Plastic limit: $w_p$	21.80%	26.10%
Plasticity index: $I_p$	14.3	5.5
Void ratio: $e$	0.551	0.731
Porosity: $n$	35.5%	42.2%
Saturated unit weight: $\gamma_{sat}$	19.5 kN/m³	19.0 kN/m³

\*Since the in-situ falling head test was conducted in the vicinity before each soil sample was collected, the result can be affected by the test, tending toward wetness.

same. So, only the result for Depth D, which is close to the slip surface, is shown. According to X-ray diffraction, the major constituent minerals are a large amount of quartz, feldspar, though a little less than quartz, and amphibole and vermiculite, though in small amounts. Although biotite was not detected, it is assumed that it had changed into vermiculite of clay mineral by weathering. Kaolin, which is a clay mineral, is a weathered product of feldspar in general, so it is considered to be

**Table 2.** Mineral contents.

Sample	Quartz	Feldspar	Amphibole
Depth D	+++ Large amount	++ Medium amount	+ Small amount
Sample	Vermiculite	Kaolin	Illite
Depth D	+ Small amount	(+) Trace amount	(+) Trace amount

**Fig. 7.** Whole rock X-ray diffraction diagram.**Fig. 8.** Preferred oriented X-ray diffraction diagram (treated by hydraulic elutriation method).

generated from a part of it because the kaolin contains much feldspar. Illite was also detected, but as shown in Utada [14], it is estimated to be a weathered clay mineral from feldspar. Due to the fact that it was estimated to be decomposed granite soil from the macroscopic examination on site and the soil test in the laboratory, the sample was found to be weathered decomposed granite soil of granodiorite, as it contained amphibole and a combination of other minerals.

Granodiorite is a plutonic rock rich in plagioclase, which is, as shown in Iida [15], Matsukura [16], and the like, characterized by forming a thick weathered layer. It is also known that biotite and feldspar gradually become fine particles when weathered, and eventually change into

clay minerals. It was found that the granodiorite of Gogoshima Island has a similar characteristic.

### 4.3. Planar Evaluation of Factor of Safety with Respect to Slope Failure in the July 2018 Heavy Rainfall

#### 4.3.1. Evaluation Method of Factor of Safety with Respect to Slope Failure

Using the simple prediction equation of rainfall seepage process shown in Section 3, the flow of rainwater underground in accordance with the flow shown in Fig. 9 was tracked and the factor of safety with respect to slope failure was attempted to evaluate. The factor of safety was calculated for each 5 m × 5 m square meshes. However, the movement of rainwater in the ground between meshes is not considered. Since the saturated hydraulic conductivity obtained from the in-situ test is close to the representative value of  $1.0 \times 10^{-3}$  cm/s of fine sand set by Ozaki et al. [7], the parameters  $\beta_v$  and  $I_{cr}$  of the simple prediction equation are set in this study as  $\beta_v = 2.05$  and  $I_{cr} = 40$  mm/hr, which are the values set by Ozaki et al. [7].

The factor of safety with respect to the slope failure  $F_s$  is calculated by using the following equation on an assumption of a semi-infinite slope, similar to the proposed condition of the simple prediction equation.

$$F_s = \frac{c + \gamma_{sat} \cdot H \cdot \cos^2 \beta \cdot \tan \phi}{\gamma_{sat} \cdot H \cdot \sin \beta \cdot \cos \beta}, \quad \dots \dots \dots (3)$$

where  $\gamma_{sat}$  is the saturated unit weight of soil (kN/m<sup>3</sup>),  $H$  is the distance from the ground surface to the wetting front (m),  $\beta$  is the dip angle of slope (°),  $c$  is the cohesion (kN/m<sup>2</sup>), and  $\phi$  is the internal friction angle (°).

In general, when calculating the factor of safety of a slope saturated with water from the slip surface to the ground surface, hydrostatic pressure acts on the slip surface. However, the state of 100% saturation in the rainfall seepage process before reaching the initial groundwater level is different from one of complete saturation that shows the hydrostatic pressure distribution. Also, in the saturated-unsaturated seepage flow analysis (FEM analysis) by Ozaki et al. [7], the pressure head is 0 m until the wetting front reaches the initial groundwater level even if the saturation is 100%, and a hydrostatic pressure distribution is not shown. The result that the pressure head also shows a hydrostatic pressure distribution has been obtained, together with the process in which the groundwater level rises rapidly to the ground surface soon after the wetting front reaches the initial groundwater level. Therefore, in this study, in the seepage process of rainfall, the soil has been saturated but buoyancy has not occurred in the soil particles, and adopted the saturated unit weight  $\gamma_{sat}$  in the calculation of the soil resistance. Note that since the soil has been saturated but buoyancy has not occurred in the soil particles, the cohesion and internal friction angle are total stress criteria.

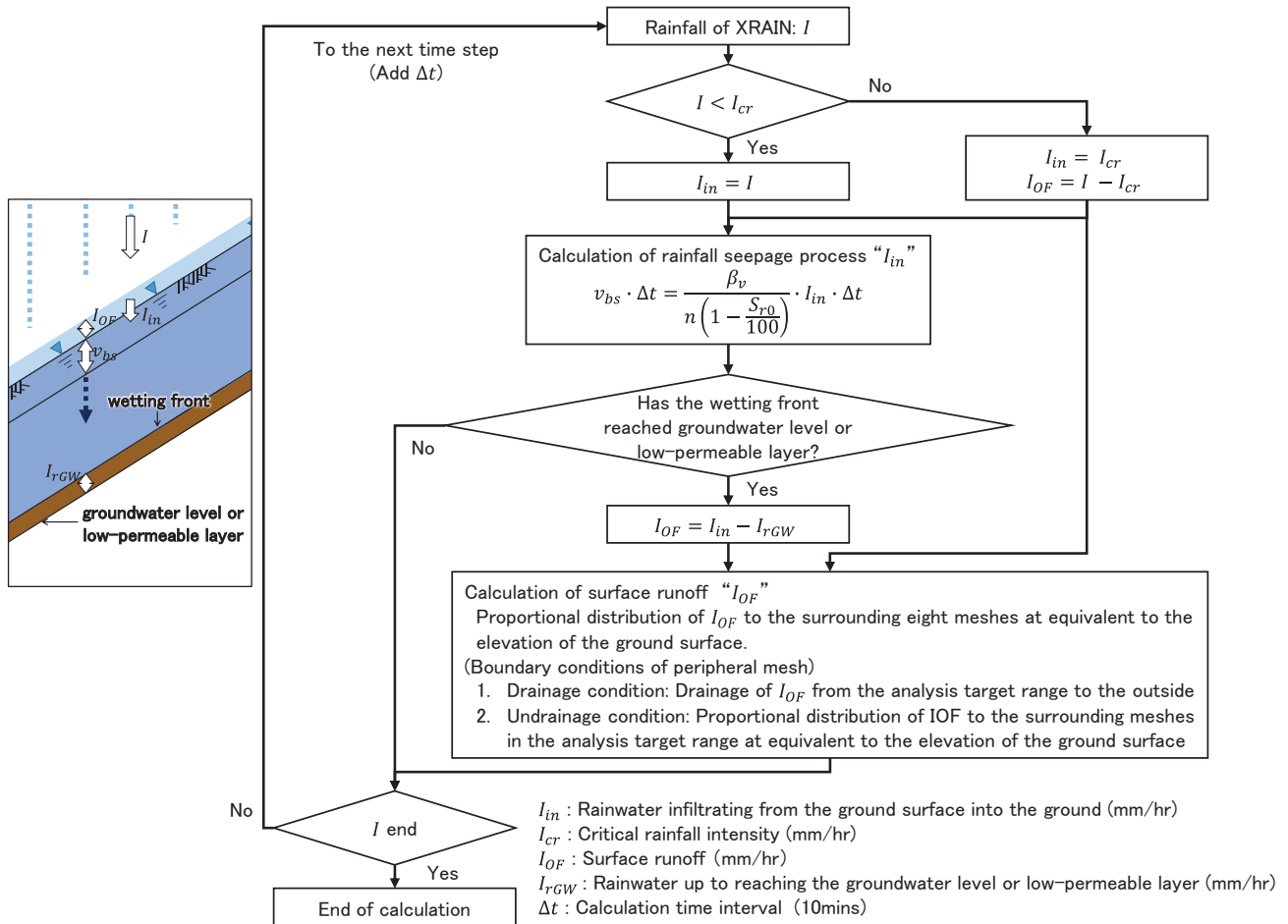


Fig. 9. Calculation flow of rainwater.

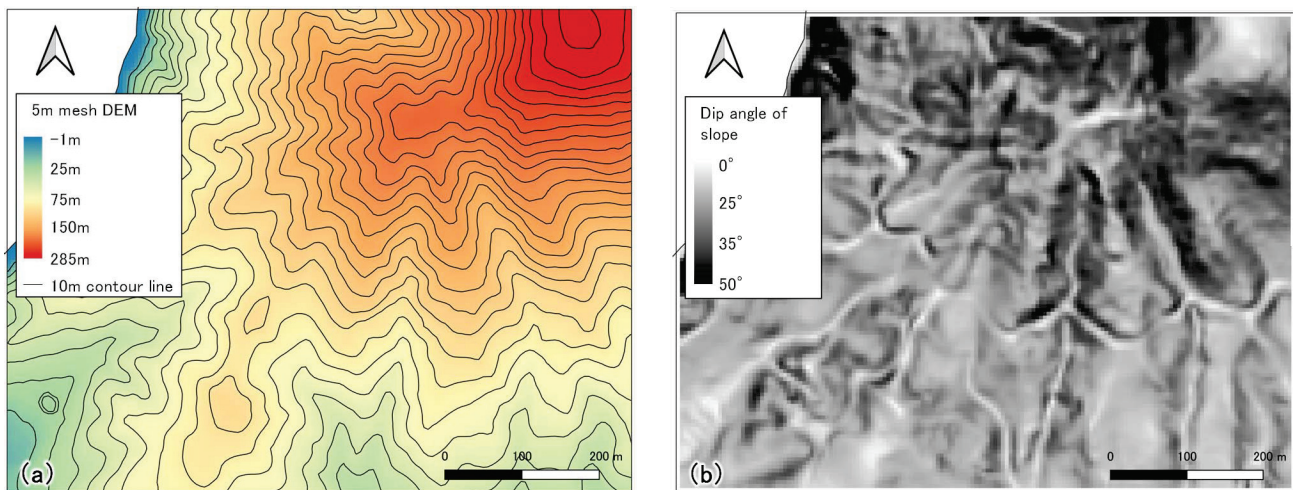


Fig. 10. (a) Elevation and (b) dip angle of slope of calculation region.

#### 4.3.2. Input Condition

As for the rainfall, XRAIN data published by the Ministry of Land, Infrastructure, Transport and Tourism [17] was adopted, and the canopy interception ratio was not considered. As for the elevation of each calculation grid defined at 5 m square, the elevation value of a 5 m mesh

DEM (work year: 2012 (before the slope failure in July 2018)) [18] from the Fundamental Geospatial Data published by the Geospatial Information Authority of Japan was adopted and interpolated by the bilinear interpolation method [19] (Fig. 10(a)). The dip angle was set by the average maximum technique [20] using this elevation data



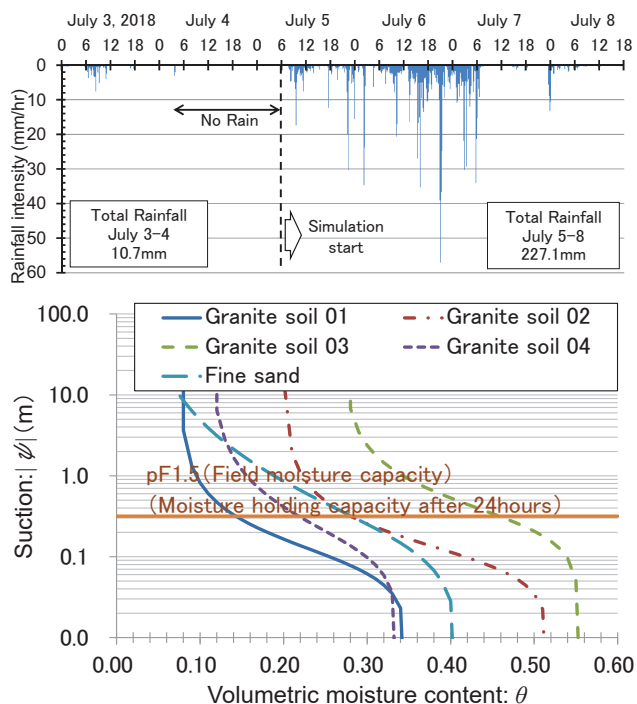


**Fig. 11.** Additional information on setting the initial saturation (see **Table 3** for various parameters).

(**Fig. 10(b)**). ArcGIS 10.8 for this series of processing was used. The calculation time interval was 10 minutes.

The porosity  $n$  and initial degree of saturation  $S_{r0}$  are required to evaluate the rainfall seepage process of a slope using the simple prediction equation. As for the porosity  $n$ , a value of 42.2% of Depth  $D$  was adopted, close to the slip surface. The initial degree of saturation  $S_{r0}$  was assumed to be 60% from the relationship between the antecedent rainfall and the no-rainfall time with respect to the analysis target rainfall (from 6:00 a.m. on July 7, 2018) of this study. This is because degree of saturation  $S_r$  equivalent to pF 1.5 is in the range of 41.1 to 82.7% as shown in **Fig. 11**, based on the moisture retention characteristics with respect to samples of decomposed granite soil and fine sand obtained from Nishigaki and Takeshita [21] in **Table 3**, on the assumption of a moisture state equivalent to a suction pressure of pF 1.5 (field moisture capacity).

As for the saturated unit weight  $\gamma_{sat}$  necessary for calculation of the factor of safety, the value of Depth  $D$  of 19.0 kN/m<sup>3</sup> was adopted from **Table 1**, similar to the setting basis of the porosity  $n$ . As for the internal friction angle  $\phi$ , Hiyama et al. [22] pointed out that the internal friction angle of unsaturated decomposed granite soil is almost constant regardless of the suction. As a result, the value of Depth  $D$  of  $\phi = 34.2^\circ$  obtained from the vane cone shear test using the soil strength probe was adopted. As for the cohesion, Hiyama et al. [22] pointed out that the cohesion of unsaturated decomposed granite soil increases linearly with an increase in suction. Araki et al. [23] pointed out that the cohesion of undis-

**Table 3.** Water retention characteristics adopted for setting initial degree of saturation and calculation result of degree of saturation equivalent to pF 1.5.

Soil type	Granite soil				Fine sand
	01	02	03	04	
$\theta_s$	0.348	0.517	0.554	0.338	0.410
$\theta_r$	0.075	0.199	0.270	0.110	0.000
$\alpha$	11.1	10.2	3.49	7	6.32
$n$	2.08	2.13	2.06	1.82	1.41
$S_{r-pF1.5}$	41.1	54.2	82.7	64.5	68.5

$\theta_s$ : Saturated volumetric moisture content

$\theta_r$ : Residual volumetric moisture content

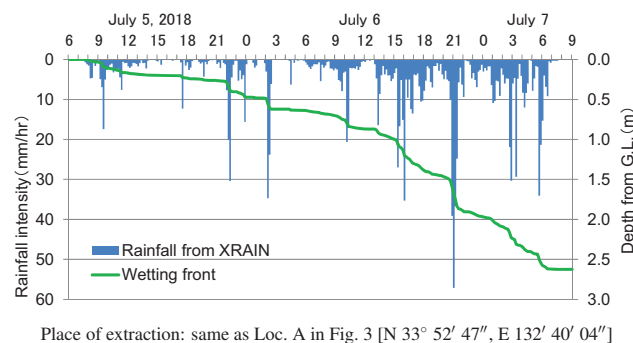
$\alpha$  (1/m),  $n$ : Parameters of van Genuchten model

$S_{r-pF1.5}$ : Degree of saturation equivalent to pF 1.5 (Moisture holding capacity after 24 hours)

\*The values of Nishigaki and Takeshita [21] were adopted for various parameters of the water retention characteristics.

**Table 4.** Each parameter used for the back calculation of cohesion.

$\gamma_{sat}$	$H$	$\beta$	$\phi$
19.0 kN/m <sup>3</sup>	1.5 m	35.0°	34.2°



Place of extraction: same as Loc. A in Fig. 3 [N 33° 52' 47", E 132° 40' 04"]

**Fig. 12.** Calculation result (location of wetting front).

turbed decomposed granite soil decreases due to water infiltration. Therefore, it is not appropriate to adopt the result of the vane cone shear test conducted in an unsaturated state. In the light of the fact that the failure depth of the source area of the slope failure in the vicinity of the test site was about 1.5 m and the dip angle was about 35° from Sato et al. [8], a back calculation of the cohesion  $c$  was performed from Eq. (3) on an assumption that the factor of safety  $F_s = 1.0$  under the conditions in **Table 4**. As a result, the cohesion  $c = 0.39$  kN/m<sup>2</sup> was given.

The physical properties of the soil shown above were given uniformly in the Depth direction. It is also assumed that there is no effect of initial groundwater.

#### 4.3.3. Planar Evaluation of Factor of Safety with Respect to Slope Failure

**Figure 12** shows the calculation result of the rainfall seepage process at Loc. A of **Fig. 3**, and **Fig. 13** shows

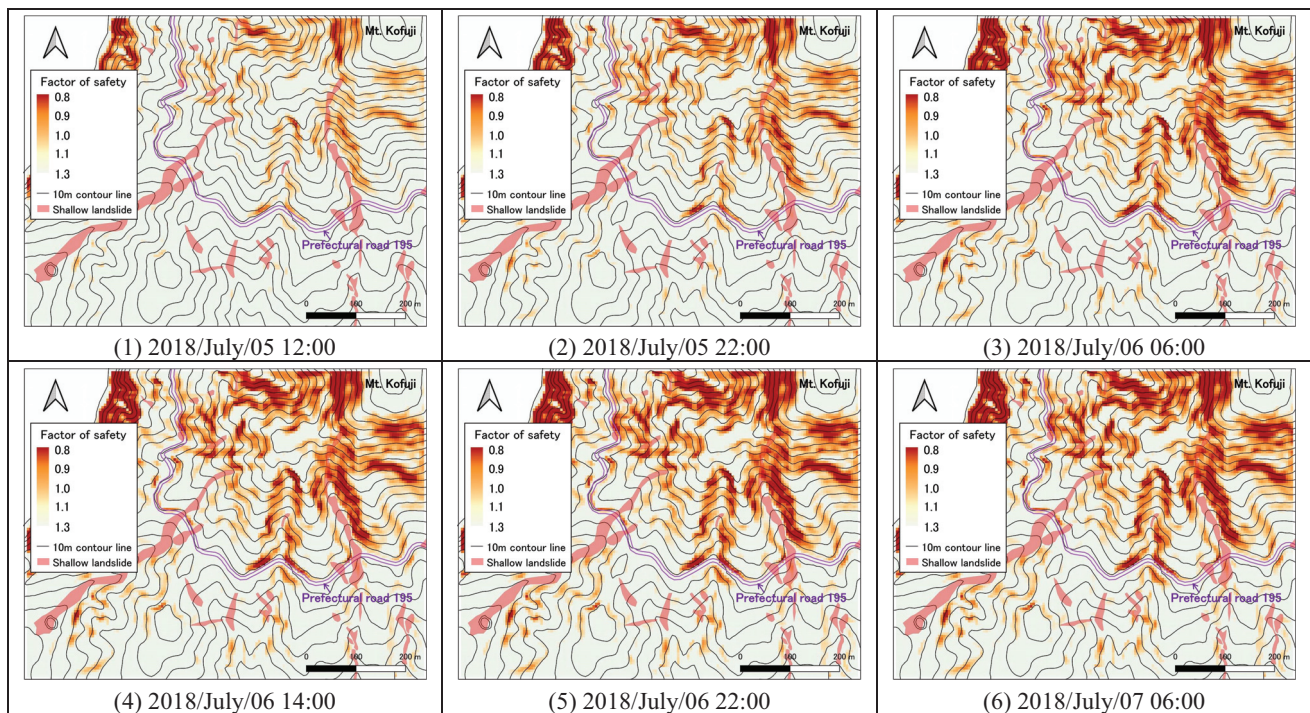


**Fig. 13.** Planar evaluation result of factor of safety with respect to slope failure.

the evaluation result of the planar factor of safety with respect to a slope failure. The areas of slope failure (red areas) due to the July 2018 heavy rains shown in **Fig. 13** includes not only the occurrence source but also flow-down, erosion and deposition areas. The factor of safety at the slope of valley head and valley wall in the upstream of the dissected valley has decreased in agreement with the area of slope failure of July 2018. As a result, the usefulness of this planar evaluation method of the factor of safety has been shown.

However, there are places where slope failure did not occur during the July 2018 heavy rains even in places where the factor of safety was evaluated to decrease over time using the simple prediction equation. This tendency is found to be seen mainly at Mt. Kofuji, which is composed of andesite, but is considered to be due to the fact that the physical properties of the decomposed granite soil of granodiorite were given uniformly and analyzed in this study. It is necessary to conduct a similar in-situ test and laboratory test in the andesite distribution area, understand the weathering characteristics and the structure of soil layer, and then evaluate the factor of safety by considering the planar difference in physical properties.

According to **Fig. 13**, there are some places around the slope failure caused by the July 2018 heavy rains for which calculation results show that the factor of safety does not decrease. The slope failure south of Prefectural Road 195 in **Fig. 13** on a relatively smooth hillside slope where the mountain was not subjected to dissection. The slope of failure was mainly a citrus field artificially modified into a staircase, as shown in **Fig. 14**. About **Fig. 14**, shown in red is distribution of slope failure caused by July

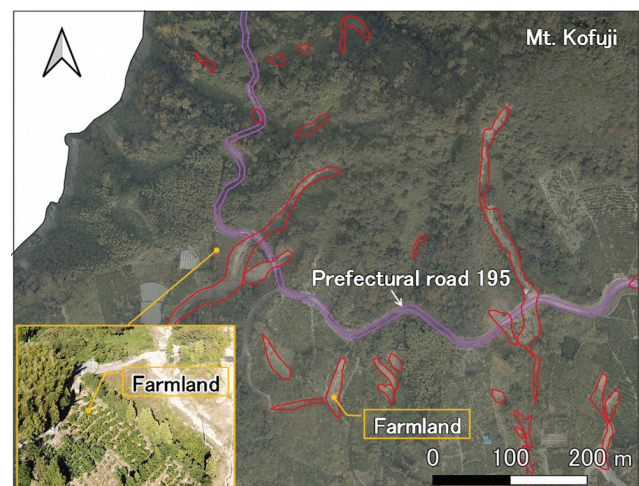


**Fig. 14.** Satellite photograph of the analysis area (Forestry Agency [9]) and an example of a citrus field artificially modified into a staircase.

2018 heavy rain (Sato et al. [8]). It was inferred that the topsoil ran off until slope failure due to the surface flow at the time of heavy rain. That is, seepage process of rainfall was not involved, and the slope failure was generated by a mechanism different from the proposed method. In addition, since the slope failure of the July 2018 heavy rains involved the flow-down, erosion, and deposition areas, it is possible that this study was not able to evaluate it similarly.



## 5. Conclusions

This study has shown that the factor of safety can be planarly evaluated with respect to the slope failure occurring in the head and wall of a valley dissecting the hillside slope using the simple prediction equation of the rainfall seepage process. This method is suitable for grasping the change tendency over time of the factor of safety for slope failure by rainfall pattern. In other words, it is possible to estimate the occurrence source of a slope failure and places with a future risk of slope failure based on real-time prediction information. However, in order to ensure early warning against human damage, it is essential to evaluate the risk while including the debris flow of the sediment supplied to the valley bottom. This study has not been able to evaluate the phenomenon in which the topsoil runs off until slope failure under surface flow at the time of heavy rains. Therefore, future challenges include adding a surface runoff calculation for the ground surface to this analysis and evaluating the sediment transport and erosion by the tractive force.

This study targeted Gogoshima Island, and it is inferred that there are islands in the Seto Inland Sea having granodiorite in which the progress of weathering is similar, from the origin of islands. Since there are many places in these islands that do not have a rescue system in case of emergency, it is important to minimize human damage as much as possible by constructing a real-time early warning judgment system for slope failure. Therefore, it is significant to develop a similar evaluation method for surrounding islands.

## Acknowledgements

Part of this research was supported by the JST Strategic International Collaborative Research Program (SICORP) e-ASIA JRP "Establishment of a Landslide Monitoring and Prediction System" (Grant Number: JPMJSC18E3). The XRAIN and surface geological data were provided by the Ministry of Land, Infrastructure, Transport and Tourism, the elevation data (5 m mesh DEM) was provided by the Geospatial Information Authority of Japan, the Ministry of Land, Infrastructure, Transport and Tourism, and the aerial laser measurement data after the disaster was provided by the Forestry Agency. Matsuyama City cooperated in collecting local information, Gunma University and its graduate school students cooperated in conducting laboratory soil tests, and Japan Conservation Engineers & Co., Ltd. cooperated in X-ray diffraction analysis. We would like to express our gratitude to all those mentioned above.

## References:

- [1] K. Okada, Y. Makihara, A. Shimo, K. Nagata, M. Kunitsugu, and K. Saito, "Soil Water Index," *Tenki*, Vol.48, No.5, pp. 349-356, 2001 (in Japanese).
- [2] Y. Ishihara and S. Kobatake, "Runoff Model for Flood Forecasting," *Bulletin of the Disaster Prevention Research Institute, Kyoto University*, Vol.29, No.1, pp. 27-43, 1979.
- [3] T. Okimura, N. Torii, Y. Osaki, M. Nambu, and K. Haraguchi, "Construction of real-time type hazard system to predict landslides caused by heavy rainfalls," *J. of the Japan Society of Erosion Control Engineering*, Vol.63, No.6, pp. 4-12, 2001 (in Japanese).
- [4] C. de Lima Neves Seefelder, S. Koide, and M. Mergili, "Does parameterization influence the performance of slope stability model results? A case study in Rio de Janeiro, Brazil," *Landslides*, Vol.14, No.4, pp. 1389-1401, 2017.
- [5] Z. Shi, F. Wei, and V. Chandrasekar, "Radar-based quantitative precipitation estimation for the identification of debris flow occurrence over earthquake-affected regions in Sichuan, China," *Nat. Hazards Earth Syst. Sci.*, Vol.18, No.3, pp. 765-780, 2018.
- [6] A. Wakai, K. Hori, A. Watanabe, F. Cai, H. Fukazu, S. Goto, and T. Kimura, "A simple prediction model for shallow groundwater level rise in natural slopes based on finite element solutions," *J. of the Japan Landslide Society*, Vol.56, No.Special-Issue, pp. 227-239, 2019 (in Japanese).
- [7] T. Ozaki, A. Wakai, A. Watanabe, F. Cai, G. Sato, and T. Kimura, "A simplified model for the infiltration of rainwater in natural slope consisting of fine sands," *J. of the Japan Landslide Society*, Vol.58, No.2, pp. 57-64, 2021 (in Japanese).
- [8] G. Sato, T. Kimura, K. Hirota, T. Ching-Ying, and H. Tagi, "Distribution of shallow landslides and related mass movement processes induced by the heavy rain in July 2018 on Gogoshima Island, Ehime Prefecture, Japan," *J. of the Japan Landslide Society*, Vol.56, No.3, pp. 129-134, 2019 (in Japanese).
- [9] Forestry Agency, Ministry of Agriculture, Forestry, and Fisheries, "Aerial laser measurement work in forest areas (Part 2) 2018," [https://www.maff.go.jp/j/budget/yosan\\_kansi/sikkou/tokutei\\_keihi/seika\\_H30/ippan/#190](https://www.maff.go.jp/j/budget/yosan_kansi/sikkou/tokutei_keihi/seika_H30/ippan/#190) (in Japanese) [accessed July 15, 2020]
- [10] K. Nagai, K. Horikoshi, M. Miyahisa, and T. Hiraoka, "1/50,000 Subsurface Geological Map and Explanatory Article of Mitsuhamma Area," Ehime Prefecture, 1975 (in Japanese).
- [11] Public Works Research Institute, "Investigation manual about soil site of slope using Soil Strength Probe," *Technical Note of Public Works Research Institute*, Vol.4176, pp. 1-40, 2010 (in Japanese).
- [12] T. Tagawa, "Simple infiltration test of surface soil," *J. of Hydrological System*, Vol.118, pp. 54-58, 2020 (in Japanese).
- [13] The Japanese Geotechnical Society, "Soil Testing (2nd Edition)," p. 17, Maruzen Publishing, 2010 (in Japanese).
- [14] M. Utada, "Alteration of Rokko Granites: Mineralogical and Magnetic Susceptibility Changes," *J. of Geography*, Vol.112, No.3, pp. 360-371, 2003 (in Japanese).
- [15] T. Iida, "Knowledge of shallow landslide and deep-seated landslide for technicians," p. 237, Kajima Institute Publishing, 2012 (in Japanese).
- [16] Y. Matsukura, "The Earth's Changing Surface – Weathering and Erosion –," p. 242, Asakura Publishing, 2008 (in Japanese).
- [17] Data Integration & Analysis System (DIAS), The University of Tokyo, "MLIT XRAIN dataset," <https://www.diasjp.net/service/xrain/> (in Japanese) [accessed September 18, 2020]
- [18] Geospatial Information Authority of Japan, MLIT of Japan, "Fundamental Geospatial Data (5m mesh DEM)," <https://fgd.gsi.go.jp/download/mapGis.php?tab=dem> (in Japanese) [accessed July 12, 2020]
- [19] Esri Japan Corporation, "Resample," <https://desktop.arcgis.com/ja/arcmap/latest/extensions/spatial-analyst/performing-analysis/cell-size-and-resampling-in-analysis.htm> (in Japanese) [accessed November 1, 2020]
- [20] Esri Japan Corporation, "Slope," <https://desktop.arcgis.com/ja/arcmap/10.3/tools/3d-analyst-toolbox/how-slope-works.htm> (in Japanese) [accessed November 1, 2020]
- [21] M. Nishigaki and Y. Takeshita, "Research on the Method of Determining Unsaturated Soil Hydraulic Properties by In-Situ or Laboratory Tests," Okayama University, 1993 (in Japanese).
- [22] H. Hiyama, M. Takayama, and T. Noda, "Shear Strength Properties of Compacted Decomposed Granite Soil," *Trans. of the Japanese Society of Irrigation, Drainage and Reclamation Engineering (JSIDRE)*, No.205, pp. 109-117, 2000 (in Japanese).
- [23] S. Araki, M. Takeuchi, N. Torii, S. Shibuya, S. Kawajiri, and S. Kagamiyama, "Strength Characteristics of Undisturbed Decomposed Granite Soil Focusing on Shear Modulus," *J. of Applied Mechanics*, Vol.13, pp. 495-502, 2010 (in Japanese).



---

**Name:**  
Takatsugu Ozaki

**Affiliation:**  
Ph.D. Student, Graduate School of Science and  
Technology, Gunma University

**Address:**  
1-5-1 Tenjincho, Kiryu, Gunma 376-8515, Japan

**Selected Publications:**  
• T. Ozaki, A. Watanabe, A. Wakai, and F. Cai, "A simple prediction  
model for shallow groundwater level rising in natural slopes based on  
finite element analysis," Geotechnics for Sustainable Infrastructure  
Development: Proc. of the 4th Int. Conf. on Geotechnics for Sustainable  
Infrastructure Development, pp. 993-1000, 2019.

---

---

**Name:**  
Akihiko Wakai

**Affiliation:**  
Professor, Gunma University

**Address:**  
1-5-1 Tenjincho, Kiryu, Gunma 376-8515, Japan

---

---

**Name:**  
Go Sato

**Affiliation:**  
Professor, Graduate School of Environmental Informations, Teikyo Heisei  
University

**Address:**  
4-21-2 Nakano, Tokyo 164-8530, Japan

---

---

**Name:**  
Takashi Kimura

**Affiliation:**  
Assistant Professor, Graduate School of Agriculture, Ehime University

**Address:**  
3-5-7 Tarumi, Matsuyama, Ehime 790-8566, Japan

---

---

**Name:**  
Takanari Yamasaki

**Affiliation:**  
Visiting Professor, Graduate School of Environmental Informations,  
Teikyo Heisei University

**Address:**  
4-21-2 Nakano, Nakano-ku, Tokyo 164-8530, Japan

---

---

**Name:**  
Kazunori Hayashi

**Affiliation:**  
Assistant Manager, Okuyama Boring Co., Ltd.

**Address:**  
13-18-306 Futsukamachi, Aoba-ku, Sendai, Miyagi 980-0802, Japan

---

---

**Name:**  
Akino Watanabe

**Affiliation:**  
Graduate Student, Geotechnical Engineering Laboratory, Department of  
Environmental Engineering Science, Gunma University

**Address:**  
1-5-1 Tenjincho, Kiryu, Gunma 376-8515, Japan

---